

A Review of Applications of Rotating and Vibrating Membranes Systems: Advantages and Drawbacks

Michel Y. Jaffrin^{1,*} and Luhui Ding²

Technological University of Compiègne, 60205 Compiègne Cedex, ¹UMR CNRS 7338; ²EA 4297 TIMR, France

Abstract: Dynamic filtration (DF) consists in creating a high membrane shear rate by disks rotating near a fixed membrane or by rotating or vibrating membranes. The shear rate can exceed $3 \times 10^5 \text{ s}^{-1}$ in some modules and significantly increases permeate flux and membrane selectivity as compared to cross flow (CF) devices. This paper describes several DF industrial modules and gives equations for calculating shear rates at rotating and vibrating membranes. It reviews 23 recent articles from 2008 to 2014, dealing with diverse applications: separation of microalgae from sea water by UF, clarification of rough beer, concentration of CaCO_3 suspensions, treatment of dairy effluents and shipboard wastewaters, inulin extraction from chicory juice, treatment of oil field water, and separation of bovine albumin from yeast. In several applications, the maximum permeate flux at initial concentration ranged from 270 to $760 \text{ Lh}^{-1} \text{ m}^{-2}$. Modules with ceramic membranes rotating around several shafts inside a housing seem to be preferable to the concept of multi-compartments modules with metal disks rotating between fixed membranes. Since the cost of DF modules is higher than that of spiral wound ones, it is better to apply DF to "end of pipe treatment" after an initial concentration by CF.

Keywords: High shear rate filtration, rotating disks, rotating or vibrating membranes.

1. INTRODUCTION

High shear rate dynamic filtration (DF) by membrane is a relatively recent concept, which generally gives better performance than cross flow filtration (CF) because high shear rates increase permeate flux and reduce membrane fouling [1-3]. In CF, to obtain a high permeate flux requires both a large fluid velocity of $4\text{-}6 \text{ ms}^{-1}$ along the membrane and a high transmembrane pressure (TMP). But a high fluid velocity creates a pressure drop which reduces the mean TMP and therefore the mean flux. In addition, the combination of high flow rates and high feed pressures requires powerful pumps which are costly and consume much energy.

DF avoids some of these limitations as the membrane shear rate is created by moving parts such as metal disks rotating at high speed between fixed membranes or by rotating cylindrical or disk membranes. Another efficient and successful concept is the VSEP (Vibratory shear-enhanced processing, New Logic Research, Ca US) proposed in 1992 by Armando *et al.* [4] which consists in vibrating azimuthally circular membranes mounted on a vertical shaft.

Advantages of DF

In addition to producing permeate fluxes 3 to 5 times higher than with CF, DF also increases solute

transmission through the membrane in microfiltration (MF) by reducing cake formation and membrane fouling [5]. In ultrafiltration (UF), nanofiltration (NF), and reverse osmosis (RO) the transfer of microsolute such as ions and small molecules into permeate is mainly diffusive and is reduced at high shear rate because their membrane concentration is lowered as they are swept away [6]. Thus, membrane rejection is higher, which is important for waste water treatment [7].

Another advantage is that DF can reduce energy consumption of the pumps, as feed flow rate needs to be only slightly higher than filtration flow rate, since the shear rate is independent of feed flow. If the goal is to maximize permeate fluxes, a high rotation speed of disks or membranes is necessary and it increases energy consumption, but since permeate fluxes are high, the specific energy per m^3 of permeate may be lower than in CF. Liberman [8] listed the advantages of the Novoflow single shaft filter: an effective cake layer control due to centrifugal forces and the presence of turbulence promoters, the decoupling of TMP from fluid velocity which permit to use low pressure of 0.2 to 2 bar which helps cleaning the membrane and increase flux performance. He also claimed that using moderate rotation speeds produces fluxes similar to CF, but with a specific energy consumption lower by 70%.

The VSEP also minimizes its energy consumption by vibrating membranes at their resonant frequency which is close to 60.75 Hz for pilots and a little less for industrial modules. It also permits to reach a high dry solid concentration of about 70% in a single pass because the feed flow rate is only slightly higher than

*Address correspondence to this author at the Technological University of Compiègne, 60205 Compiègne Cedex, UMR CNRS 7338, France; Tel: +33 4423 4398; Fax: +33 4420 4813; E-mail: michel.jaffrin@utc.fr

permeate flow. Rotating disks modules such as the Dyno from Bokela GmbH (Germany) with compartments connected in series can also reach high solid concentrations without recirculation.

Drawbacks

The most obvious drawback of DF modules is their complexity, especially for those with rotating disks or rotating membranes, which increases construction and maintenance costs. Another drawback is the limited membrane area of some modules, 2.3 m² for the Spintek (USA), 5 m² for the CRD from Novoflow (Germany) and 8 m² for the Dyno. Due to their cost, DF systems may not be competitive when large membrane areas are required, but they are well adapted to “end of pipe” treatment, using a first CF concentration step with spiral wound modules to reduce retentate volume,

which is then treated by DF to reach high concentrations.

2. INDUSTRIAL MODULES OF DYNAMIC FILTRATION

Present industrial modules may be classified in 3 types, a) metal disks or blades rotating between fixed circular membranes (Rotating disk module, RDM) like the Dyno and the Optifilter, circular polymeric or ceramic membranes rotating between fixed plates like the Spintek (USA), b) ceramic membrane disks rotating around parallel shafts inside a housing, c) vibrating membranes like the VSEP.

Rotating Disks and Membranes Systems

The Dyno with disks rotating between fixed membranes (Figure 1) is commercialized by Bokela

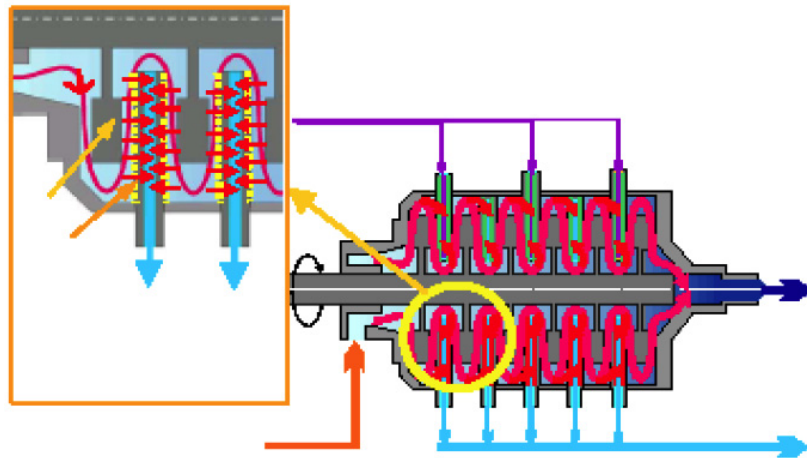


Figure 1: Dyno module with disks rotating between fixed circular membranes (Bokela, Germany).



Figure 2: Spintek module with rotating membranes.

(Germany) with membrane area up to 8 m². It can be equipped with polymer or ceramic membranes. Its maximum pressure of 600 kPa limits its use to MF and UF. The Spintek, shown in Figure 2, is available with up to 10 polymer or ceramic membranes rotating around a shaft between fixed disks forming compartments. The maximum membrane area is 2.3 m² and pore size ranges from 0.07 μ to 3 μ, covering UF and MF, with a maximum pressure of 150 psi, or 14.5 bar. A Korean company commercializes a module with fixed circular membranes separated by veined disks acting as vortex generators, the FMX shown in Figure 3, which can receive MF, UF, NF and RO membranes. Its applications are metal removal, winery stillage, distillery and methylcellulose wastewater treatment.

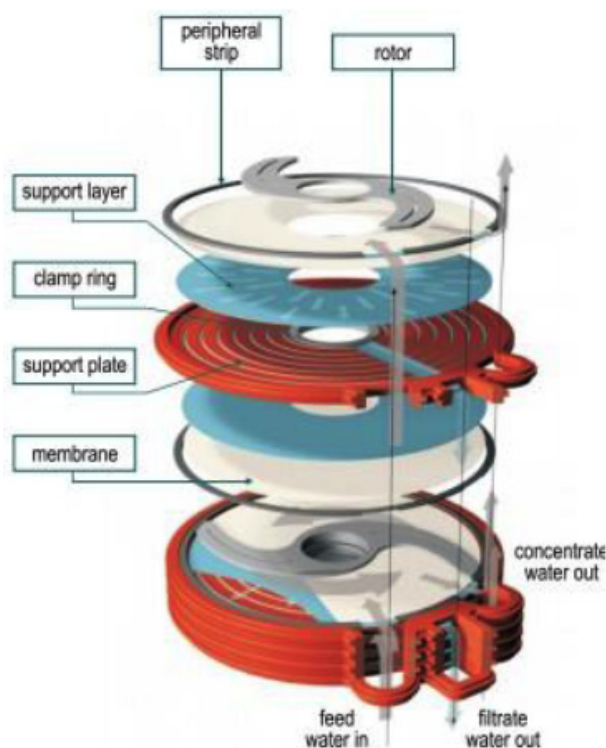


Figure 3: Module structure and industrial equipments of OptiFilter CR, Metso Paper Co.

Other DF systems are available with membrane area above 140 m², such as the Optifilter (Metso Paper, Finland) [9], shown in Figure 4, which uses blades mounted on a vertical shaft, rotating between fixed circular flat membranes of up to 1 m diameter. Smaller units of 15 and 84 m² are also available. Andritz KMPT Co (Germany) proposes a two shafts module with overlapping ceramic disks with membrane areas from 2 to 10 m² with pore sizes from 7 nm to 0.4 μ. The circumferential speed at rim is 7.3 ms⁻¹. Another German Company, Novoflow, commercializes two

single shaft modules with rotating ceramic membranes, the CRD with a 5 m² membrane area for MF and UF and the SSDF with 31 cm diameter MF, UF and NF membranes of 25 m² total area.

Vibrating Membrane Systems

The most successful system is the VSEP composed of a stack of circular organic membranes mounted on a vertical shaft separated by gaskets. A VSEP lab pilot is shown in Figure 5. The shaft base vibrates in azimuthal oscillations with amplitude of 2 to 3 cm at membrane rims at its resonant frequency of 60.75 Hz. The use of resonance minimizes the power consumed by the vibrations at only 9 kW for systems of 150 m² membrane area, which are shown in Figure 6. These various modules can generate very high shear rates at membrane, up to 1.2 10⁵ s⁻¹ produced by the inertia of retentate without large feed flow rates and pressure drops and the resulting low solute concentration at the membrane reduces concentration polarization and membrane fouling. The VSEP can sustain pressures of 40 bar and operates efficiently in NF and RO.

The vibration concept has also been applied to hollow fiber cartridges, shaken longitudinally, but the shear rate is lower than in the VSEP, as the vibration amplitude is smaller.

3. SHEAR RATE CALCULATIONS IN DF MODULES

Calculations of membrane shear rates permit to predict modules performances and can be found in the literature. For a disk or a rotor of radius R_d rotating near a stationary membrane of radius R, the averaged shear rate over the membrane area in turbulent regime is given by [3]

$$\gamma_{tm} = 0.0164 (k\omega)^{1.8} R^{1.6} v^{-0.8} = 0.55 \gamma_{max} \quad (1)$$

where γ_{max} is the maximum shear rate at disk rim ($r=R_d$), ω is the disk angular velocity, v is the kinematic viscosity and k is a velocity coefficient such that $k\omega$ is the fluid angular velocity at membrane. This coefficient was measured to be 0.42 for a flat disk, and is at least 0.82 when the disk is equipped with eight 6 mm high radial vanes [10-11]. Thus shear rates at disk rim can easily reach 3-4 10⁵ s⁻¹ at large rotation speed.

In the case of rotating membranes mounted on a single shaft, as in the Spintek, the mean membrane shear rate for turbulent flows is given by [12]

$$\gamma_{tm2} = 0.0317 \omega^{1.8} R^{1.6} v^{-0.8} \quad (2)$$

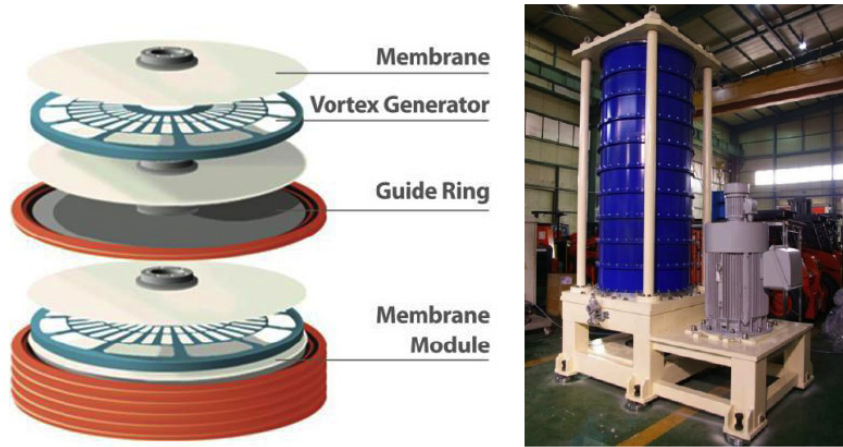


Figure 4: Module structure and industrial equipment of FMX system, BKT.

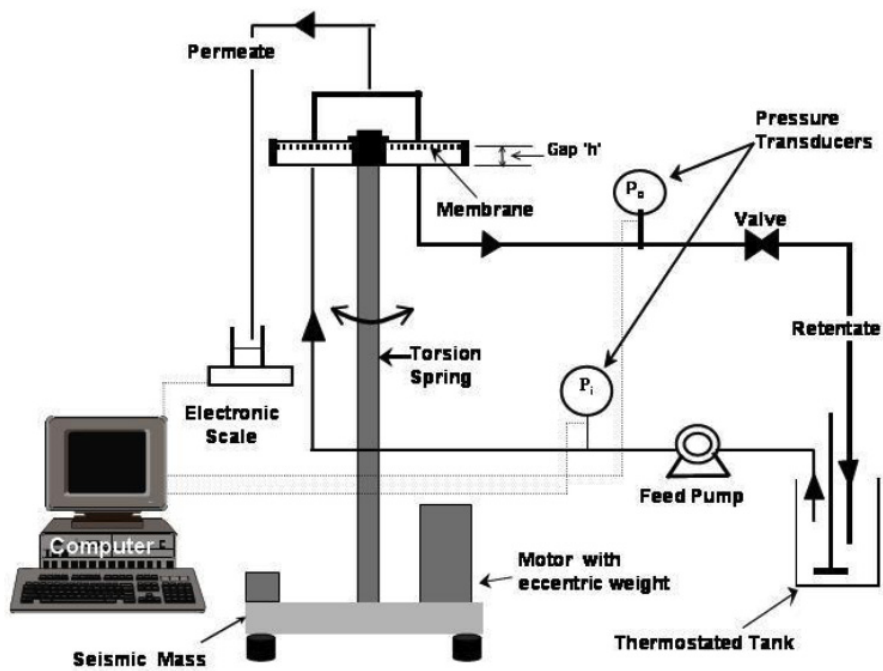


Figure 5: Schematic of VSEP pilot series L with a single membrane, oscillating around its vertical axis.



Figure 6: Industrial VSEP vibrating modules (Courtesy of New Logic Research).

It is higher than for a disk rotating near a fixed membrane.

The membrane shear rate in VSEP systems varies with time and radius. Its maximum with time at the disk periphery is given by Al Akoum *et al.* [13]

$$\gamma_{\max 1} = 2^{0.5} d_1 (\pi F)^{1.5} v^{-0.5} \quad (3)$$

where d_1 is the membrane displacement at periphery depending upon frequency F . It is smaller, at about 10^5 s^{-1} for water and $d_1 = 3 \text{ cm}$ than membrane shear rates in a RDM of same diameter at speed above 900 rpm [14].

4. REVIEW OF RECENT APPLICATIONS

4.1. Applications of Rotating Disks and Membranes Systems

Frappart *et al.* [15] investigated the influence of hydrodynamics in CF and dynamic ultrafiltration for microalgae separation from sea water. The CF module was a Rayflow 100 (Orelis, France) with a rectangular membrane of 100 cm^2 fed by a 180 Lh^{-1} feed flow and the UTC (University of technology of Compiègne) RDM module had a metal disk with radial vanes, rotating at 360 rpm near a fixed circular membrane of 188 cm^2 fed with only 30 Lh^{-1} . This low rotation speed was selected to produce the same mean shear rate of 16000 s^{-1} in both devices. The membrane was a PAN 40 kDa, the TMP and the temperature were respectively 1 bar and 25°C in both devices. At $\text{VRR}=1$, the RDM flux decreased from 140 to $70 \text{ Lh}^{-1}\text{m}^{-2}$ after 140 min while the Rayflow flux decreased from 160 to $40 \text{ Lh}^{-1}\text{m}^{-2}$ in the same time. During concentration tests, permeate fluxes decayed while the VRR increased to 3, but the RDM permeate flux decayed from $100 \text{ Lh}^{-1}\text{m}^{-2}$ to 78 against only 58 to $35 \text{ Lh}^{-1}\text{m}^{-2}$ for the Rayflow. This flux difference can be explained by the laminar regime of the Rayflow and the turbulent regime of RDM due to presence of radial vanes. This result confirms the gain in flux obtained from turbulent regime at the same shear rate.

Fillaudeau *et al.* [16] clarified rough beer with a rotating and vibrating filtration module (RVF) equipped with a three blades impeller of 142 mm diameter rotating between two flat MF membranes fixed on porous plates to drain the permeate. Its membrane area was 0.048 m^2 and the gap between blades and membranes was 3 mm. Its rotation speed varied from 600 to 3000 rpm and membrane pore size from $0.6 \text{ }\mu\text{m}$ to $4 \text{ }\mu\text{m}$. The special blade geometry produced TMP

variations which vibrated membranes and increased mass transfer and filtration flux. The steady state flux at 4°C increased with TMP and pore size to reach a maximum flux of $270 \text{ Lh}^{-1}\text{m}^{-2}$ with the $1.10 \text{ }\mu\text{m}$ pore membrane at 2.5 bar, while the flux was limited to about $80 \text{ Lh}^{-1}\text{m}^{-2}$ with $0.80 \text{ }\mu\text{m}$ and $0.6 \text{ }\mu\text{m}$ pores. The authors concluded that, although yeast cells were responsible for a strong fouling above $\text{VRR} > 10$, it was not critical and the RVF gave a higher flux than CF.

Sarkar *et al.* [17] described an original module in which a 30 kDa membrane mounted on a disk rotates next to a contra-rotating rotor disk. They applied it to protein recovery from casein whey. They obtained, at a TMP of 686 kPa and a rotation speed of only 300 rpm, an initial flux of $500 \text{ Lh}^{-1}\text{m}^{-2}$, which stabilized to $252 \text{ Lh}^{-1}\text{m}^{-2}$ after 20 min of filtration. They probably could have increased this flux using a higher rotation speed.

Tamner and Ripperger [18] compared the performance of a MSD (multishaft disk) pilot in single and double shaft configurations in order to see if overlapping membranes could increase the flux. The test fluid was a suspension of $10 \text{ }\mu\text{m}$ glass spheres. They observed that the permeate flux would drop with increasing rotation speed because of centrifugal forces acting on permeate side. At a TMP of 7 kPa, and a rotation speed of 740 rpm, the permeate flux remained stable at $1925 \text{ Lh}^{-1}\text{m}^{-2}$ in two shaft configuration, while with one shaft the flux decayed from $2200 \text{ Lh}^{-1}\text{m}^{-2}$ to $400 \text{ Lh}^{-1}\text{m}^{-2}$ after 10 min and decayed slowly after that to $300 \text{ Lh}^{-1}\text{m}^{-2}$ after 1 hr. Such high fluxes are due to the nature of the tested fluid which does not induce fouling. Authors concluded that the double shaft configuration permitted a stable operation at moderate speed.

Tu and Ding [19] used a MSD laboratory pilot with 12 overlapping ceramic membrane disks rotating at same speed on two parallel horizontal shafts to concentrate a CaCO_3 suspension. They modified the pilot by replacing the ceramic disks on upper shaft by nylon membranes with same $0.2 \text{ }\mu\text{m}$ pore size fixed on porous disks by a metal ring. Figure 7 compares permeate fluxes for nylon membranes rotating at 1930 rpm and a TMP of 250 kPa, reaching $840 \text{ Lh}^{-1}\text{m}^{-2}$ with those of ceramic ones reaching only $760 \text{ Lh}^{-1}\text{m}^{-2}$. It also presents the variation of permeate flux with TMP with membranes rotating at 738 rpm and metal disks rotating at speeds from 738 to 1930 rpm. These metal disks increased the flux of nylon membranes by a factor of 3 for a maximum of $1723 \text{ Lh}^{-1}\text{m}^{-2}$ versus $593 \text{ Lh}^{-1}\text{m}^{-2}$ without metal disks (no m.d), while the

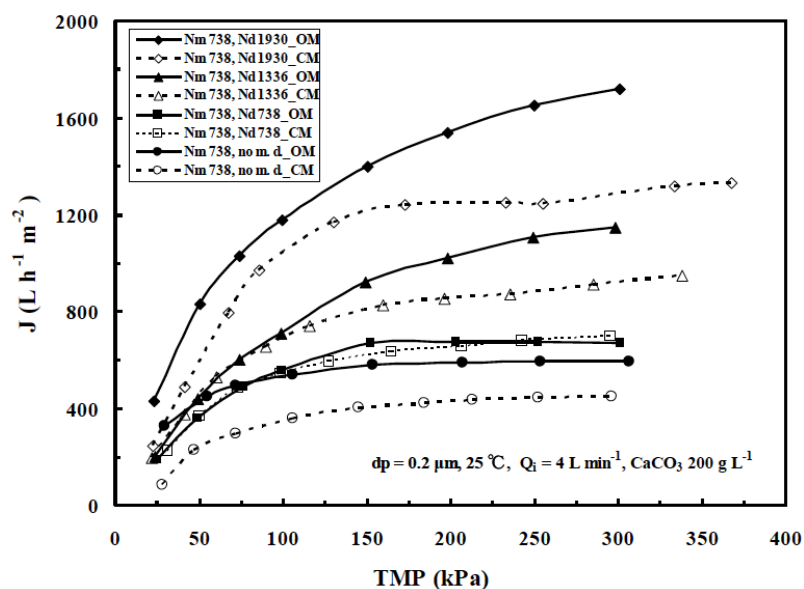


Figure 7: Variation of permeate flux with TMP with membrane disks rotating at 738 rpm and metal disks with vanes rotating at various speeds Nd from 738 to 1930, for both organic (OM) and ceramic (CM) membranes. From [19] with permission.

maximum flux of ceramic membranes was $1300 \text{ Lh}^{-1}\text{m}^{-2}$. This was due to the high permeability of nylon membrane, $5180 \text{ Lh}^{-1}\text{m}^{-2}\text{bar}^{-1}$ against $704 \text{ Lh}^{-1}\text{m}^{-2}\text{bar}^{-1}$ for ceramic disks. However, the flux advantage of nylon membranes was offset by their higher energy consumption with a maximum of 2.9 kWh m^{-3} , due to friction caused in part by the fixation ring and by their lower membrane area, against 1.7 kWh m^{-3} for ceramic disks.

Luo *et al.* [20] used a RDM lab pilot equipped with a NF 270 membrane to treat a model dairy wastewater composed of milk diluted to one third initial concentration. They carried out two long terms batch tests at 2000 rpm with a total duration of 17 h per test, spread over 7 days at a TMP of 40 bar. Results of these tests are shown in Figure 8. During the 1st test with chemical cleaning at a pH of 10 (Figure 8a), the permeate flux decayed slowly from $430 \text{ Lh}^{-1}\text{m}^{-2}$ to 360 . With alkaline cleaning at pH=11 during the 5th day, the flux rose a little, but decayed to $260 \text{ Lh}^{-1}\text{m}^{-2}$ due to pores fouling. During the 2nd test without chemical cleaning (Figure 8b), the flux dropped rapidly from $360 \text{ Lh}^{-1}\text{m}^{-2}$ to 180 after 3 hr and rose again to $350 \text{ Lh}^{-1}\text{m}^{-2}$ after water rinse. These tests confirmed that, with frequent chemical cleaning, a high and stable flux of about $320 \text{ Lh}^{-1}\text{m}^{-2}$ was possible, while water rinsing cannot remove fouling and, in this case, the flux dropped from 275 to $170 \text{ Lh}^{-1}\text{m}^{-2}$ in 2 hr, even at high shear rate.

In another article, Luo *et al.* [21] proposed a new concept of threshold flux in shear-enhanced NF of

model dairy effluents (skim milk diluted 1:2). They defined it as the flux at which the flux-TMP relationship becomes nonlinear. This flux was determined by pressure-stepping tests when reversible fouling was stable. When operating above threshold flux at 35°C (Figure 9a) the permeate flux decayed slowly from $430 \text{ Lh}^{-1}\text{m}^{-2}$ at 2000 rpm and 40 bar to $389 \text{ Lh}^{-1}\text{m}^{-2}$ after 350 min. However, in 2nd test, the membrane decayed faster after 300 min. Figure 9b shows that the flux remained high and stable after cleaning, but, if fouled membranes were only rinsed with warm water, their flux was lower and decayed rapidly after 30 min. The authors estimated that an initial flux above threshold flux was preferable as the foulant-deposited-foulant interaction can be investigated.

Bendick *et al.* [22] used a high shear HSR-MS rotating membrane system with $0.06 \mu\text{m}$ pores to treat shipboard wastewaters (bilge and black water). Pressurized feed entered the cylindrical housing while permeate crossed the ceramic membrane of 267 mm diameter and discharged into the hollow shaft. The concentrate was returned to a 400 L feed tank. Authors measured mean permeate fluxes over three concentric areas, of respective diameters $198 < d < 229 \text{ mm}$ for outer region, $127 < d < 178 \text{ mm}$ for middle region and $76 < d < 127 \text{ mm}$ for inner one. These permeate fluxes for black water increased linearly with rotation speed from 100 to 1150 rpm. The maximum flux was $390 \text{ Lh}^{-1}\text{m}^{-2}$ at 1150 rpm for the turbulent outer region and dropped to $200 \text{ Lh}^{-1}\text{m}^{-2}$ for the laminar inner region. Fluxes were higher for bilge and reached a maximum of $440 \text{ Lh}^{-1}\text{m}^{-2}$

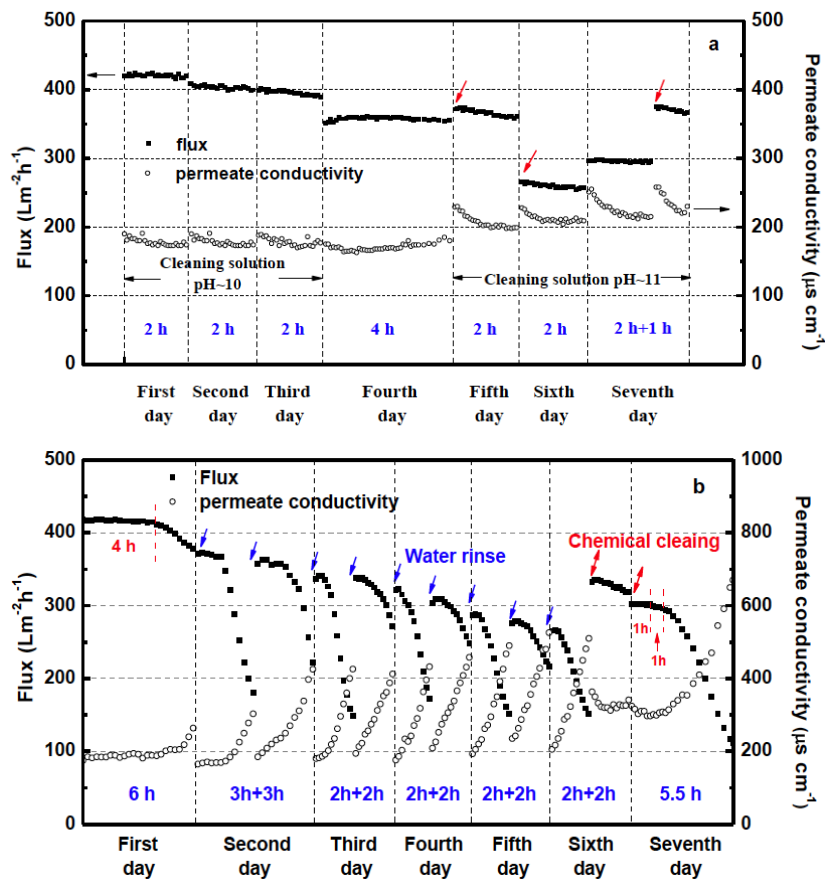


Figure 8: Permeate flux and conductivity in 7 days long-term batch filtrations with (a) or without (b) chemical cleaning. Rotating speed= 2000 rpm. From [20] with permission.

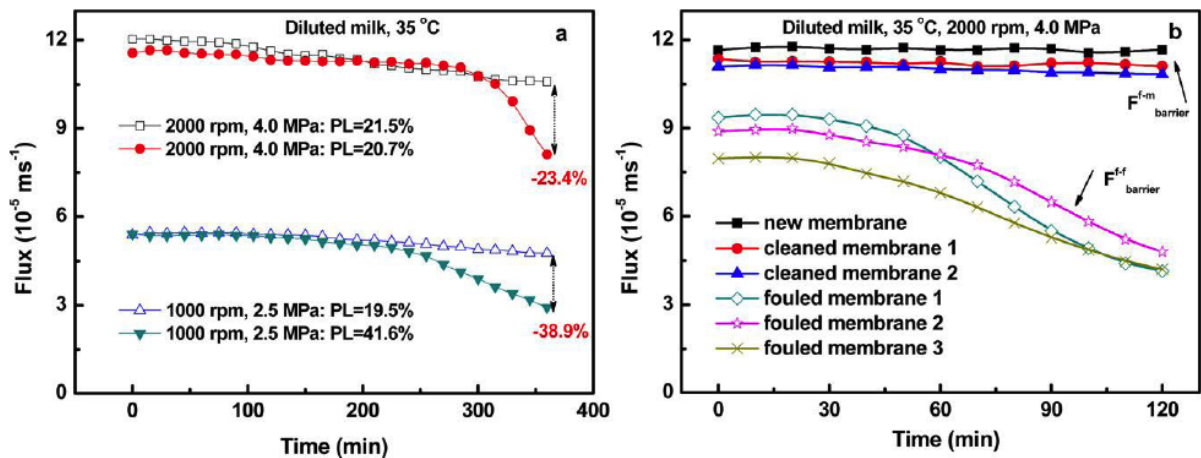


Figure 9: Permeate fluxes using diluted milk as function of time when operating above threshold flux. a) With new NF270 membranes; b) With used membranes cleaned by alkaline solution at pH=11. With fouled membranes only rinsed by warm water. From [21] with permission.

at 1150 rpm in the outer region. The authors concluded that large disks rotating at low speed can produce larger permeate fluxes than smaller disks at high speed.

Zhu *et al.* [23] clarified chicory juice to extract inulin using a RDM equipped with radial vanes and compared

its results with an Amicon 800 cell stirred at 350 rpm in dead end filtration. They compared four membranes of pores sizes of 100 kDa, 0.15, 0.2 and 0.45 μm in both modules. The steady flux of Amicon cell was about 26 $\text{Lh}^{-1}\text{m}^{-2}$ at 100 kDa and increased little with MF membranes. Variations of RDM permeate flux with

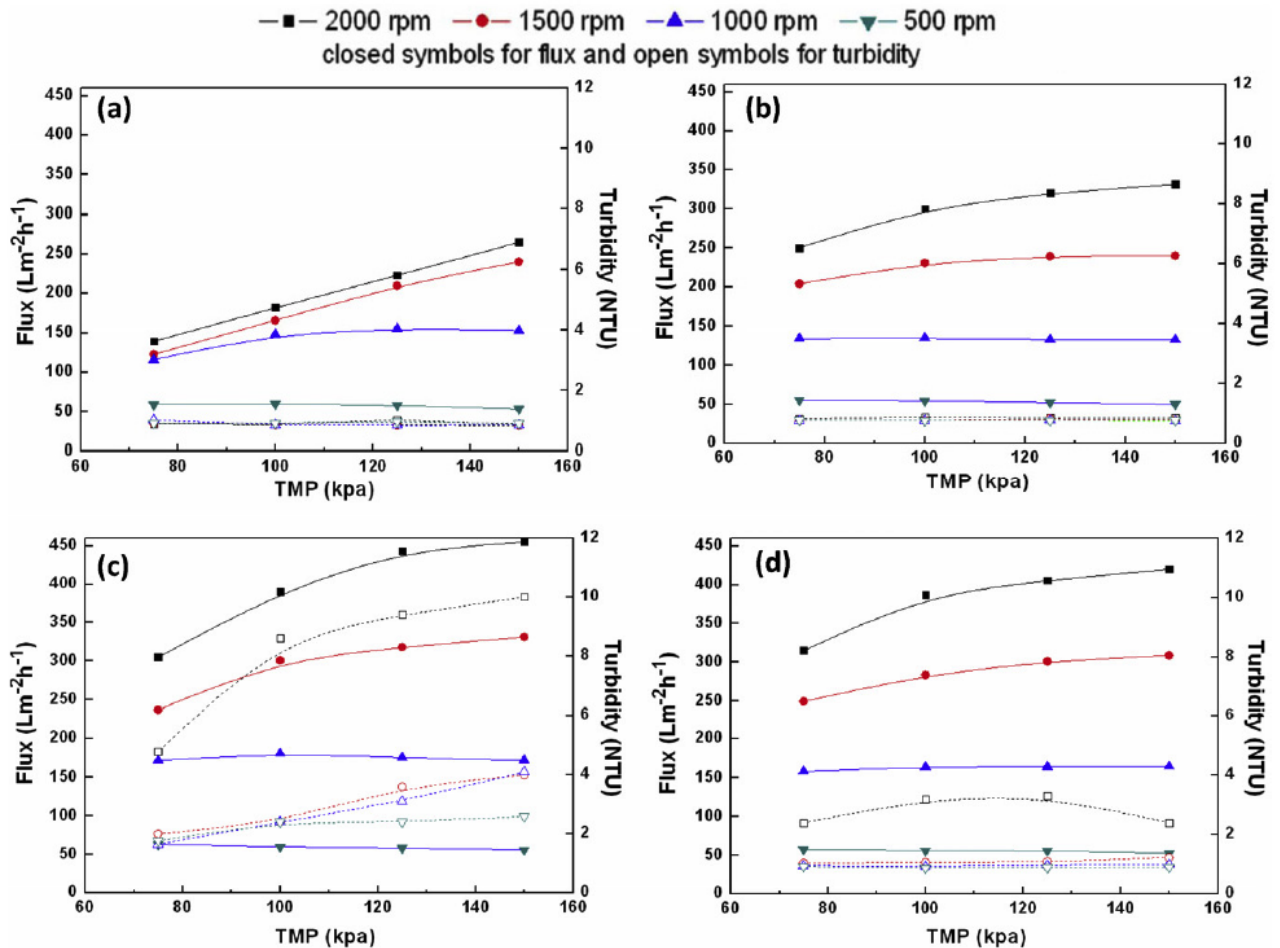


Figure 10: Chicory juice fluxes and permeate turbidity variation with TMP for four membranes (a) US100P, (b) FSM0.15PP, (c) MV020T and (d) FSM0.45PP. From [23] with permission.

TMP at various rotating speeds are displayed in Figure 10. Surprisingly, highest fluxes were obtained at 2000 rpm using the 0.2 μm membrane with $450 \text{ Lh}^{-1}\text{m}^{-2}$ at 150 kPa, against $420 \text{ Lh}^{-1}\text{m}^{-2}$ for the 0.45 μm membrane. Turbidities remained low and constant at 1 NTU for the 100 kDa and 0.15 μm membranes, but they increased with TMP to 4 NTU for the 0.2 μm membrane, which must have the best permeability and explains its largest flux. In concentration tests at 2000 rpm with the 0.45 μm membrane, the flux reached a maximum of $200 \text{ Lh}^{-1}\text{m}^{-2}$ at a VRR of 2 and decayed to $105 \text{ Lh}^{-1}\text{m}^{-2}$ at VRR=10, while permeate turbidity rose to 7 NTU.

In another paper, Zhu *et al.* [24] used the same modules in UF of chicory juice at 50 kDa. The RDM had a flux decline of only 63% versus 81% for the Amicon cell, as the radial vanes on the disk increased the shear rate and turbulence. They compared permeate fluxes with the RDM at 500 rpm, 1200 rpm and 1670 rpm, at successive TMP of 2, 4, and 6 bar. Curiously enough, highest steady fluxes at 1670 rpm

were obtained at 4 bar with $170 \text{ Lh}^{-1}\text{m}^{-2}$ and at 2 bar with $160 \text{ Lh}^{-1}\text{m}^{-2}$ against only $75 \text{ Lh}^{-1}\text{m}^{-2}$ at 6 bar. The authors attributed this unexpected result to the compaction of the solutes layer on the membrane at 6 bar. They optimized the RDM performances with a 3D response surface and reported that the optimal mean flux was $173 \text{ Lh}^{-1}\text{m}^{-2}$, obtained at a TMP of 2.9 bar and a rotation speed of 1670 rpm, with a shear rate of $102\,000 \text{ s}^{-1}$. They could have augmented the permeate flux by increasing the speed at 2000 rpm or more, but at the expense of higher energy consumption.

Ebrahimi *et al.* [25] treated oil-field produced water by MF and UF using a rotating disk filter (CRD, Novoflow) equipped with 0.2 μm and 7 nm pores ceramic disks of 152 mm diameter. At a rotating speed of 1800 rpm, a TMP of 1 bar, a temperature of 50°C and a feed concentration of 30 ppm, the permeate flux in MF concentration tests decayed from $490 \text{ Lh}^{-1}\text{m}^{-2}$ at initial concentration to $110 \text{ Lh}^{-1}\text{m}^{-2}$ after 1400 min at a VRR of 24. Oil and TOC (Total organic carbon) rejection were quite high at 99% and 98% respectively

and independent of rotation speed. In UF under 1800 rpm, the initial flux was $275 \text{ Lh}^{-1}\text{m}^{-2}$ and decayed to $225 \text{ Lh}^{-1}\text{m}^{-2}$ after 10 h at a VRR of 15. At 1200 rpm, the flux was only $125 \text{ Lh}^{-1}\text{m}^{-2}$ at a VRR of 15, confirming the benefit of higher rotation speed. Oil and TOC rejections were the same as in MF.

In an interesting paper, Zhang *et al.* [26] investigated the effect of hydraulic conditions on treatment of model dairy effluents (milk diluted to 1/3) using a Box-Behnken response surface methodology, with the same RDM pilot used by Zhu *et al.* [22]. They ran 15 tests with a 30 kDa membrane at rotation speeds from 750 to 2250 rpm, TMP from 2 to 7 bar, feed flows from 60 to 120 L/h. Test 12 at 2250 rpm, 7 bar and a feed flow of 90 L/h, minimized permeate COD at 6.9 mg/L and protein concentration at 1.04 mg/L. Test 6 at 750 rpm, 4.5 bar and 120 L/h maximized permeate COD at 8.4 mg/L and protein concentration at 3.31 mg/L. The highest decline happened in test 10 with 21.7% at 750 rpm, 7 bar and 90 L/h. Table 1 lists the characteristics of selected tests. A comparison of tests 3 and 4 shows that doubling the feed flow only increased the flux from 125 to $136 \text{ Lh}^{-1}\text{m}^{-2}$. Test 9, at 750 rpm and 2 bar, minimized permeate quality and permeate flux ($37 \text{ Lh}^{-1}\text{m}^{-2}$) and maximized flux decline (20%). A comparison of tests 4 with tests 8 and 10 showed that a high TMP (7 bar) increased the flux more than a large rotation speed, but, at low speed (750 rpm), flux decline was high. Test 11, at 2250 rpm and 2 bar gave the lowest flux ($57 \text{ Lh}^{-1}\text{m}^{-2}$), but the smallest flux decline, 4.0%. Test 12, at 7 bar and 2250 rpm gave the best compromise between high flux and low flux decline, respectively $128 \text{ Lh}^{-1}\text{m}^{-2}$ and 6.8%. The authors also calculated the specific energy consumption per m^3 of permeate. The lowest value occurred in test 10 with 130 kWhm^{-3} . The highest was 770 kWhm^{-3} for test 11. The best compromise between high permeate fluxes and moderate energy consumption could be test 4 which produced the

highest average flux of $136 \text{ Lh}^{-1}\text{m}^{-2}$ with a consumption of 182 kWh m^{-3} at 1500 rpm.

Luo *et al.* [27] investigated the clarification of chicory juice using a RDM and the same membranes as in [23], a 100 kDa UF and three MF ones with 0.15, 0.2 and $0.45 \mu\text{m}$ pores. They plotted permeate fluxes at a TMP of 75 kPa as a function of rotation speed in Figure 11a for each membrane. Highest fluxes were obtained at the maximum speed of 2000 rpm for the $0.45 \mu\text{m}$ membrane ($318 \text{ Lh}^{-1}\text{m}^{-2}$) and for the $0.2 \mu\text{m}$ one ($307 \text{ Lh}^{-1}\text{m}^{-2}$), against $139 \text{ Lh}^{-1}\text{m}^{-2}$ for the UF membrane between 1000 and 1500 rpm. The variation of specific energy consumption per m^3 of permeate with rotation speed, plotted in Figure 11b, was minimum for the $0.2 \mu\text{m}$ and $0.45 \mu\text{m}$ membranes and equal to 100 kWh m^{-3} between 1000 and 1500 rpm. The flux variation with TMP was plotted in Figure 12a in order to determine the threshold flux, corresponding to the end of linear flux variation with TMP, before limiting flux in for three 100 kDa membranes. This threshold flux varied from 130 to $140 \text{ Lh}^{-1}\text{m}^{-2}$ while the limiting flux varied from 149 to $155 \text{ Lh}^{-1}\text{m}^{-2}$. Figure 12b describes three strategies, the 1st consisted in operating at 50 kPa and $125 \text{ Lh}^{-1}\text{m}^{-2}$ below threshold flux. The 2nd operated above threshold flux with a flux decaying from $160 \text{ Lh}^{-1}\text{m}^{-2}$ to 150 after 300 min and the 3rd corresponded to a limiting flux at 120 kPa decaying from 150 to $136 \text{ Lh}^{-1}\text{m}^{-2}$ after 300 min. The authors concluded that operating at threshold flux and 1000 rpm minimized fouling flux decline, and that increasing rotation speed for short periods at 2000 rpm permitted to remove the fouling layer.

Rios *et al.* [28] used a two-shaft DCF KMPT module with 6 overlapping ceramic membranes of 0.14 m^2 total area to harvest microalgae for biofuel. They obtained very high initial fluxes of $780 \text{ Lh}^{-1}\text{m}^{-2}$ for small algae, *Nannocloropsis gaditana* (Nng) and *Chaetoceros calcitrans* (Chc) using $0.5 \mu\text{m}$ pore size at 1.6 bar and 1150 rpm. They set up an economic study and found

Table 1: Characteristics of Selected Runs from [26]

Run	Feed flow L/h	TMP bar	N rpm	Flux J $\text{Lh}^{-1}\text{m}^{-2}$	Flux decline %
3	60	7	1500	125	15.6
4	120	7	1500	136	16.4
8	120	4.5	2250	102	7.4
10	90	7	750	108	21.7
11	90	2	2250	57	4.5
12	90	7	2250	128	6.8

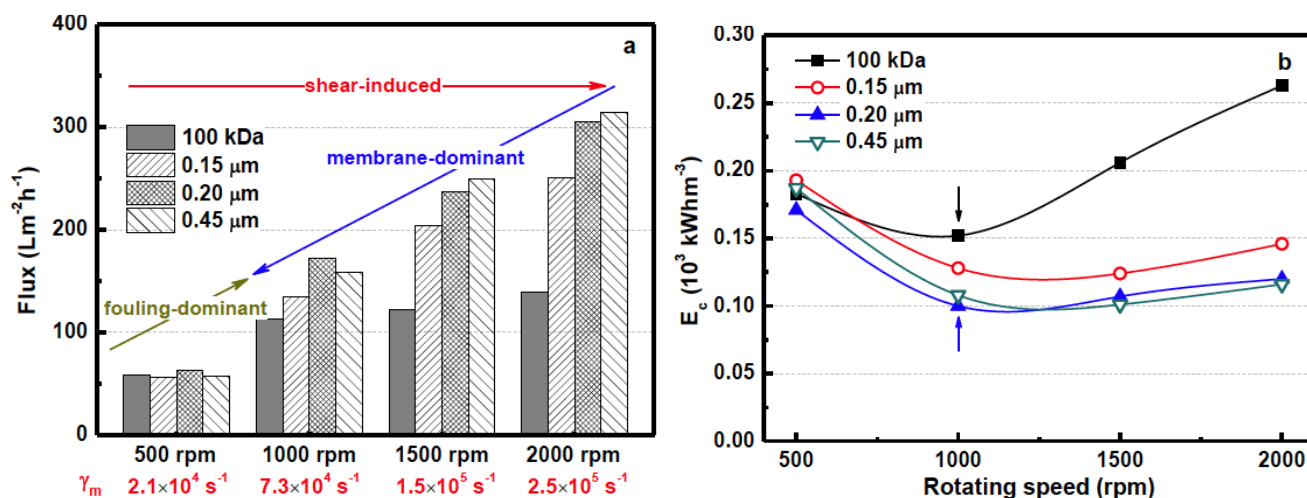


Figure 11: Effect of rotating speed on (a) permeate flux and (b) specific motor energy consumption for different membranes at TMP=75 kPa in a 1st series of experiments, From [27] with permission.

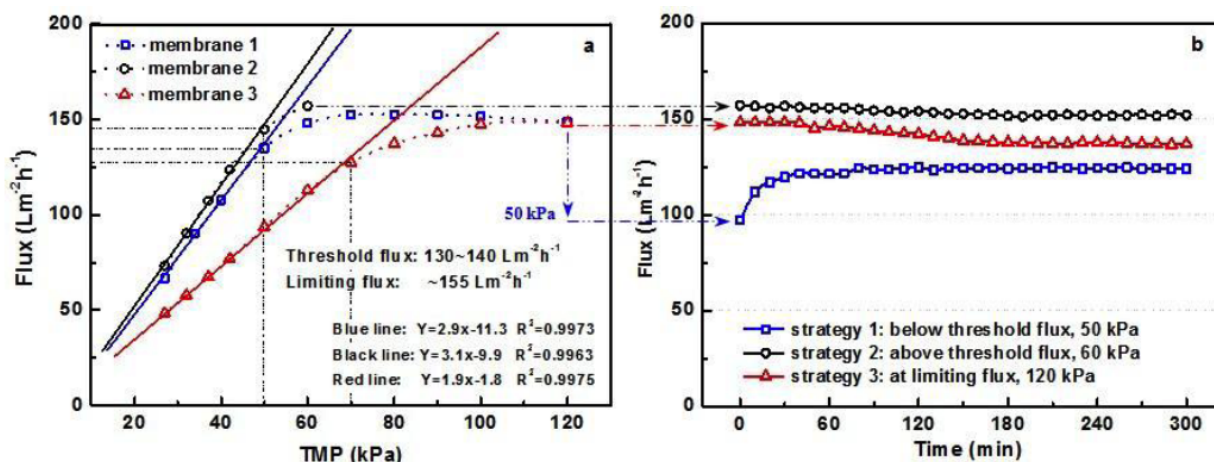


Figure 12: Permeate flux versus TMP (a) and versus time at constant TMP operations for 100 kDa membranes in a 2nd series of experiments. From [27] with permission.

that the cost of dry biomass decayed with increasing flux from 0.65 \$/ kg at 80 Lh⁻¹m⁻² to 0.4 \$/kg at 140 Lh⁻¹m⁻². They concluded that adding a sedimentation step before the DF microfiltration reduced the overall cost of dry biomass to 0.0077\$/kg.

4.2. Applications of Vibrating Membranes

Shi and Benjamin [29] investigated the effect of shear rate on fouling in a VSEP pilot for concentrating brackish water and brine by RO. The permeate flux of brackish water at a TMP 965 kPa decayed from 46 Lh⁻¹m⁻² at start to 20 at a recovery of 90% (VRR=10). With brine, the flux decayed from 23 Lh⁻¹m⁻² to 2.5 Lh⁻¹m⁻² at a recovery of 80%. The flux decay was mainly due to the osmotic pressure which rose from 48 kPa to 448 kPa at 90% recovery for brackish water and to 827 kPa at 75% recovery for the brine. The authors confirmed the importance of vibration amplitude on permeate flux

which dropped at 40% recovery from 14 Lh⁻¹m⁻² at a vibration amplitude of 15.9 mm to 8.6 Lh⁻¹m⁻² at 0.32 cm. These low fluxes are due to small vibrations amplitudes which are normally close to 25 mm.

Ahmed *et al.* [30] used a VSEP pilot to remove arsenite AS (III) and arsenate AS (V) from drinking water with two NF membranes, a Toray UTC-70 and a Nitto Denko polysulfone NTR-745 using concentration tests at a TMP of 310 kPa and with only a 13 mm vibration amplitude. AS (V) removal rose from 90% to 100% when retentate reached 150 L with the Toray membrane. With the NTR membrane the removal rose from 80% to 84%. Due to a shear rate of 0.6 10⁵ s⁻¹ the flux was limited to 30 Lh⁻¹m⁻². When the vibration amplitude was the normal value of 25 mm, removal with UTC-70 membrane reached 100% for arsenate and 85% for arsenite and the flux stabilized at 50 Lh⁻¹m⁻². But with the NTR membrane, AS (III) removal was

limited to 27%. An increase of pH to 11 increased AS (III) to 90% with the UTC-70 membrane and to 55% with the NTR membrane. Authors concluded that process optimization should take into account raw water pH, arsenic concentration and shear rate.

Zouboulis and Petala [31] treated landfill leachates using successively a 0.1 μm MF membrane, two UF ones of 100 kDa and 10 kDa, and a NF one with 50% salt rejection. The goal was removal of organic load (COD) of suspended and dissolved solids. Initial and steady state permeate fluxes, at a vibration amplitude of 25.4 mm corresponding to a membrane shear rate of 50000 s^{-1} , were respectively 400 and $192\text{ Lh}^{-1}\text{m}^{-2}$ for MF, 200 and $146\text{ Lh}^{-1}\text{m}^{-2}$ at 100kDa, 100 and $90\text{ Lh}^{-1}\text{m}^{-2}$ at 10 kDa and 50 and $40\text{ Lh}^{-1}\text{m}^{-2}$ in NF. The MF and 100 kDa membranes gave a 95% recovery against 90% for the 10 kDa and NF membranes. COD removal was 61% in MF, 70% in UF and 90% in NF. The authors attributed these results to the high shear rate, at 30 mm vibration amplitude. They concluded that combining a 1st MF or UF step with a final NF step could be an efficient alternative.

Subramani *et al.* [32] used a VSEP to further concentrate brackish water with high silica content, which had been previously treated with a spiral wound RO module. Permeate fluxes reached $100\text{ Lh}^{-1}\text{m}^{-2}$ with the VSEP as the high shear rate reduced colloidal silica deposition. Authors also observed that flux decline, which was 50% after 1.5 h of filtration at a pH of 7.4, was reduced to only 5.7% after 5h when pH was set to 5.0 by adding acid. Moreover, cleaning the membrane with a basic cleaner completely restored the initial flux, while an acid cleaner only restored it to 40%.

Kertesz *et al.* [33] investigated the performance of a VSEP L-pilot using successively a UF 7 kDa polyethersulfone membrane, and two polyamide ones, a NF 240 Da and a RO 50 Da to purify dairy wastewater. Curiously the flux was maximum in NF at $116\text{ Lh}^{-1}\text{m}^{-2}$, against $74\text{ Lh}^{-1}\text{m}^{-2}$ for UF and $42\text{ Lh}^{-1}\text{m}^{-2}$ for RO with a vibration amplitude $d_1 = 25.4\text{ mm}$. Without vibrations, these fluxes were respectively $68.5\text{ Lh}^{-1}\text{m}^{-2}$ for NF, $55\text{ Lh}^{-1}\text{m}^{-2}$ for UF and $31.6\text{ Lh}^{-1}\text{m}^{-2}$ for RO. With vibrations, COD rejections were 40% for UF, 90.5% for NF and 98.6 for RO. At $d_1 = 0$, COD rejections were respectively 27.8%, 87.4% and 98.4%. The specific energy consumption per m^3 of permeate with vibrations decayed in UF from 2.1 kWhm^{-3} at $\text{TMP} = 0.6\text{ MPa}$ to 1.82 kWhm^{-3} at 1.6 MPa. In NF, this energy was constant at 2.5 kWhm^{-3} while it decayed in RO from 4.5 kWhm^{-3} at 1.5 MPa to a minimum of 4.2 kWhm^{-3} at 2.5

MPa. Without vibrations the specific energy was lower in RO at all TMP. The higher flux of NF membrane was due in part to the higher TMP, 2 MPa against 0.8 for the UF membrane.

Gomaa *et al.* [34] tested a small dynamic filtration pilot consisting in a rectangular vertical membrane oscillating up and down for MF of baker yeasts. The displacement amplitude was varied between 3 and 30 mm and the frequency between 5 and 25 Hz. They observed that the permeate flux increased more rapidly with frequency F than with amplitude d_1 , which is consistent with (3) as the shear rate in this case is proportional to d_1 and to $F^{1.5}$. The permeate flux at a concentration of 3gL^{-1} reached a steady state of $190\text{ Lh}^{-1}\text{m}^{-2}$ for $F = 25\text{ Hz}$ and $d_1 = 3\text{ mm}$. At $F = 10\text{ Hz}$ and $d_1 = 30\text{ mm}$, the steady state flux was $148\text{ Lh}^{-1}\text{m}^{-2}$. The authors compared their results with those of Brou *et al.* [10] and Al Akoum *et al.* [13] and found that their pilot gave slightly higher fluxes. The same authors [35] added turbulent promoters to their oscillating membrane and found it reduced membrane fouling from 65% to 45% at a frequency of 20 kHz, but the reduction was small below 5Hz. The permeate flux with and without promoters at 25 kHz dropped rapidly during the first 1000 s but stabilized after 1600 s and reached $14 \cdot 10^{-5}\text{ ms}^{-1}$ with promoters against 5.6 ms^{-1} without promoters. But it is true that turbulence promoters cannot be inserted in all DF modules. In [35], promoters are parallel linear obstacles perpendicular to the flow. No promoters seem to have been proposed for rotating membranes or RDM.

Beier and Jonsson [36] used a vibrating bioreactor containing a hollow fibers cartridge oscillating at 20 Hz with an amplitude of 1.37 mm to separate bovine albumin from yeast cells. They obtained a 84% transmission for a 4 g/L BSA solution containing 8 g/L of baker yeast cells. The maximum flux was $40\text{ Lh}^{-1}\text{m}^{-2}$ due to the small vibration amplitude. This confirms the difference between VSEP performances using a 2.6 cm amplitude and those of hollow fibers oscillating at low frequency and small amplitude.

Yang *et al.* [37] presented an interesting review of shear-induced techniques to enhance liquid separation by using vibrating hollow fibers or fibers cartridges with baffles acting as turbulence promoters to create better mixing. An advantage of hollow fibers is their high surface/volume ratio (m^2/m^3) which may reach 10 000, versus 600 to 800 for spiral wound modules and 350 to 500 for plate and frame modules. The introduction of fabric woven inside the module provides a more

uniform spacing and increases the mass transfer inside fibers. They also discussed other mass transfer enhancing mechanisms like bubbling, vibrations and ultrasonic waves. They reported that the most active approach to avoid fouling inside fibers is air bubbles which induce liquid motion and promote shear rates. Air sparging in a membrane bioreactor provides aeration and creates a two-phase flow to control fouling.

5. DISCUSSION

We have selected recent articles in our review of DF applications with 23 articles from 2008 to 2014 in order to follow latest developments in DF.

Table 2 presents a synthesis of maximum fluxes obtained at initial concentration with various modules and fluids. [15] showed that, at the same low shear rate of 16000 s^{-1} and in same conditions, the RDM flux was 72% higher than that of CF Rayflow at $VRR=1$ and 2.1 times higher at $VRR=3$ and its decline was 22% in DF against 40 % in CF. The reason was that flow was

turbulent in DF with a RDM equipped with vanes, while it was laminar in Rayflow. References 16 to 31 obtained very large fluxes, especially for the MSD [19] when ceramic membranes were replaced by metal disks with vanes on one shaft, as it increased the shear rate. In [20] the RDM obtained a very high flux in NF at 2000 rpm at 40 bar ($430\text{ Lh}^{-1}\text{m}^{-2}$), because the flux kept increasing with TMP until 40 bar in NF. In [23], the low flux of $70\text{ Lh}^{-1}\text{m}^{-2}$ was due to a low TMP of 2 bar and a moderate rotation speed. In [25], the high flux of the Novoflow module ($490\text{ Lh}^{-1}\text{m}^{-2}$) was due to a 50°C temperature, a small feed oil concentration of 30 ppm, a rotation speed of 1800 rpm and a 304 mm diameter, which produced a very large shear rate. Gomaa *et al.* [33] dealt with vibrating hollow fibers and obtained a flux of $190\text{ Lh}^{-1}\text{m}^{-2}$ at a frequency of 25 Hz and a vibration amplitude of 30 mm, much larger than in similar modules with only 3 mm vibration amplitude.

One must keep in mind that fluxes listed in Table 2 were measured at initial concentration, at the start of filtration and cannot be sustained during production. It

Table 2: Synthesis of Maximum Permeate Fluxes Obtained in Reviewed Articles [15-34] Using Different Modules and Conditions

Ref	Module	Fluid	Membrane	TMP, bar	Temp °C	Max flux $\text{Lh}^{-1}\text{m}^{-2}$	Rotation speed, rpm or frequency	Diam mm
[15]	RDM Rayflow	Micro Algae suspension	40 kDa	1bar	25	100 58	360	152
[16]	RVF	Beer	1.1 μm	2.5	4	270	3000	142
[18]	MSD	Glass sphere	0.2 μm	0.07		1925	740	90
[19]	MSD	CaCO_3	0.2 μm	2.5	25	760	1937	90
[20]	RDM	Diluted milk	NF	40	35	430	2000	152
[22]	HSR-NS	Shipboard wastewater	0.06 μm	1.9	20	390	1150	241
[23]	RDM	Chicory juice	150 kDa	2.0	20	136	1000	152
[25]	CRD Novoflow	Oil field water	0.2 μm	1.0	50	490	1800	304
[26]	RDM	Diluted milk	50 kDa	7	35	130 (mean)	2000	152
[27]	RDM	Chicory juice	0.45 μm	0.75	25	318	2000	152
[31]	VSEP	Leachates	μm 100kDa	7 17	20	400 200	60 Hz 60 Hz	300 300
[33]	VSEP	Dairy wastewaters	240Da NF	20	50	116	60 Hz	300
[34]	Hollow fibers	Baker yeast	0.22 μm	0.6	22	190	25 Hz	

is clear that combining high TMP and high shear rates will generate high fluxes. Rotating metal disks with radial vanes will enhance turbulence and shear rate. A 300 mm diameter membrane rotating at 2000 rpm can produce shear rates of at least $4 \cdot 10^5 \text{ s}^{-1}$, while, in the case of vibrating membranes, shear rates seem to be limited to $1.2 \cdot 10^5 \text{ s}^{-1}$ as vibration amplitude in industrial use is limited to about 2.7 mm in a VSEP or 1.37 mm at 20 Hz in hollow fibers [34], which according to (3) should give a shear rate of about 10^4 s^{-1} . But the VSEP increases turbulence at membrane surface and reduces the vibration energy by operating near resonance frequency. It is clear that vibrating hollow fibers cartridges cannot compete with the VSEP as their vibration amplitude is much smaller than that of VSEP at rim.

Since many authors have reported the high permeate fluxes and membrane selectivity of dynamic filtration in MF, UF, NF and RO, their industrial acceptance is now growing, as European manufacturers, Bokela, Andritz KMPT, Canzler, Novoflow, Metso Paper, Spintek and New Logic Research (US) sell dynamic filtration modules. DF gives a choice between producing permeate fluxes three to five times larger than in CF at high TMP with slightly higher energy consumption per m^3 of permeate, or operating at similar fluxes as CF, but with up to 70% energy saving [8]. In both cases, the filtration cost per m^3 of fluid in DF should be less than in CF as a high permeate flux will reduce the membrane size of DF modules and their cost, while at moderate flux, DF modules need a smaller fluid velocity which reduces pumping energy. Unfortunately, sales statistics are difficult to obtain. New Logic Research Inc listed in 2014 on their site (www.vsep.com/industries/index.html) a fairly extensive list of applications on wastewater treatment (Biogas effluent, pesticide and radioactive wastewater, landfill leachate etc..) and chemical processing (Carbon, colloidal, pigment concentration, metal hydroxide filtration etc..).

6. CONCLUSION

The DF potential of high permeate fluxes and solutes transmission in MF and UF and of high flux and microsolute rejection in NF and RO has been confirmed by many investigators. There are three types of DF modules; the first consists in metal disks rotating between fixed circular membranes such as the Dyno and the UTC RDM, the second uses ceramic disks rotating around one or several parallel shafts inside a housing and the third concerns vibrating membranes

such as circular membranes oscillating azimuthally around a vertical shaft such as the VSEP, or hollow fibers cartridges vibrating vertically. The advantage of ceramic membrane disks rotating inside housing is that their construction and maintenance should be simpler, since there are no separate compartments. If membranes are mounted on several shafts, they can overlap and increase shear rate in the overlapping region, as observed in [19]. The VSEP has been quite successful as it can minimize vibrations energy by the use of resonance and, with 50 cm diameter membranes, its membrane area can exceed 150 m^2 and its maximum shear rate can reach $1.5 \cdot 10^5 \text{ s}^{-1}$ at rim. Vibrating membrane cartridges do not seem to be yet available in large size, but they should be less expensive to build than other DF modules.

Bokela GmbH praises the high permeate flux of its rotating disks modules, while Andritz KMPT and Novoflow companies emphasize energy saving at shear rates between $3 \cdot 10^4$ and $6 \cdot 10^4 \text{ s}^{-1}$ because of reduction in pump power, the high retentate solid concentration achieved in single pass and the more uniform TMP which optimizes membrane efficiency. Constraints of industrial production also limit performances of DF modules in order to avoid costly maintenance.

It is clear that the cost of DF modules per m^2 of membrane is higher than that of spiral wound modules, so they may not be advantageous for initial treatment of large fluid volumes. It is thus better to apply them to "end of pipe" treatment when the fluid has been first concentrated by CF to a moderate VRR, in order to reduce treated fluid volume and membrane area of DF modules. It is also possible in wastewater treatment by DF, to replace a RO membrane by a NF one which will have a similar rejection and a higher flux. The use of DF modules with NF and RO membranes is presently limited, but their number should increase in the future as their benefits in terms of flux and selectivity higher than in MF and UF due to a combination of high shear rates and TMP. The availability of 30 or 50 cm diameter ceramic disks in MSD, KMPT and Novoflow modules should permit this development, as it is simpler and less expensive to build such modules than multi-compartment systems with metal disks rotating between fixed membranes.

ACKNOWLEDGEMENTS

This article could not have been written without the contributions of our former PhD students, R. Bouzerar,

A. Brou, O. Akoum, M. Frappart, N. Moulai-Mostefa, Z. Tu, J. Luo, Zhu Z., X. Zhang. We also thank Veolia Waters, France and Aafrow, Germany for their gift of a VSEP and a MSD pilots, and Alting, NovaSep, and Osmonics Co for supplying membranes.

LIST OF SYMBOLS AND ABBREVIATIONS

d	= diameter, m
d_1	= vibration amplitude, m
J	= permeate flux, $Lh^{-1}m^{-2}$
L	= length, m
R	= Rd radius, disk radius, m

Greek Symbols

γ	= shear rate, s^{-1}
ν	= kinematic viscosity, L^2t^{-1}
ω	= angular velocity, rad/s

Abbreviations

CF	= crossflow filtration
COD	= carbon oxygen demand
DF	= dynamic filtration
MF	= microfiltration
MPa	= mega Pascal
RDM	= rotating disk module
TMP	= transmembrane pressure (Pa or bar)
VRR	= volume reduction ratio

REFERENCES

- [1] Lee SA, Russoi BG, Buckland B. Microfiltration of recombinant yeast cells using a rotating disk dynamic filtration system. *Biotech Bioeng* 1995; 48: 386-400. <http://dx.doi.org/10.1002/bit.260480411>
- [2] Dal-Cin MM, Lick CN, Kumar A, Lealess S. Dispersed phase back transport during ultrafiltration of cutting oil emulsions with a spinning disc geometry. *J Membr Sci* 1998; 141: 165-81. [http://dx.doi.org/10.1016/S0376-7388\(97\)00304-9](http://dx.doi.org/10.1016/S0376-7388(97)00304-9)
- [3] Bouzerar R, Ding LH, Jaffrin MY. Local permeate flux-shear-pressure relationships in a rotating disk microfiltration module: implications for global performance. *J Membr Sci* 2000; 170: 127-41. [http://dx.doi.org/10.1016/S0376-7388\(99\)00348-8](http://dx.doi.org/10.1016/S0376-7388(99)00348-8)
- [4] Armando AD, Culkin B, Purchas DB. New separation system extends the use of membranes. *Proc. Euromembrane 92*, Paris vol. 6, Lavoisier 1992; p. 459.
- [5] Bouzerar R, Jaffrin MY, Ding LH, Paullier P. Influence of geometry and angular velocity on performance of a rotating disk filter. *AIChE J* 2000; 46: 257-65. <http://dx.doi.org/10.1002/aic.690460206>
- [6] Brou A, Ding LH, Jaffrin MY. Dynamic microfiltration of yeast suspensions using rotating disks equipped with vanes. *J Membr Sci* 2002; 197: 269-82. [http://dx.doi.org/10.1016/S0376-7388\(01\)00642-1](http://dx.doi.org/10.1016/S0376-7388(01)00642-1)
- [7] Frappart M, Akoum O, Ding LH, Jaffrin MY. Treatment of dairy process waters modelled by diluted milk using dynamic nanofiltration with a rotating disk module. *J Membr Sci* 2006; 282: 465-72. <http://dx.doi.org/10.1016/j.memsci.2006.06.005>
- [8] Liebermann F. Dynamic crossflow filtration with Novoflow's single shaft disk filters. *Desalin* 2010; 250: 1087-90. <http://dx.doi.org/10.1016/j.desal.2009.09.114>
- [9] Mänttari M, Vitikko K, Nystrom M. Nanofiltration of biologically treated effluents from the pulp and paper industry. *J Membr Sci* 2006; 272: 152-60. <http://dx.doi.org/10.1016/j.memsci.2005.07.031>
- [10] Brou A, Ding LH, Jaffrin MY. Dynamic microfiltration of yeast suspensions using rotating disks equipped with vanes. *J Membr Sci* 2002; 197: 269-82. [http://dx.doi.org/10.1016/S0376-7388\(01\)00642-1](http://dx.doi.org/10.1016/S0376-7388(01)00642-1)
- [11] Torras C, Pallares J, Garcia-Valls R, Jaffrin MY. CFD simulation of a rotating disk flat; membrane module. *Desalin* 2006; 200: 453-5. <http://dx.doi.org/10.1016/j.desal.2006.03.365>
- [12] Murkes J, Carlsson CG. *Crossflow filtration*. John Wiley & Sons 1988.
- [13] Al-Akoum O, Jaffrin MY, Ding LH, Paullier P, Vanhoutte C. An hydrodynamic investigation of microfiltration and ultrafiltration in a vibrating membrane module. *J Membr Sci* 2002; 197: 37-52. [http://dx.doi.org/10.1016/S0376-7388\(01\)00602-0](http://dx.doi.org/10.1016/S0376-7388(01)00602-0)
- [14] Jaffrin MY, Ding L, Akoum O, Brou A. A hydrodynamic comparison between rotating disk and vibratory dynamic filtration systems. *J Membr Sci* 2004; 242: 155-67. <http://dx.doi.org/10.1016/j.memsci.2003.07.029>
- [15] Frappart M, Massé A, Jaffrin MY, Pruvost J, Jaouen P. Influence of hydrodynamics in tangential and dynamic ultrafiltration systems for microalgae separation. *Desalin* 2011; 235: 279-83. <http://dx.doi.org/10.1016/j.desal.2010.07.061>
- [16] Fillaudeau L, Boissier B, Moreau A, Blanpain Avet P, Ermolaev S, Jitariouk N, Gourdon A. Investigation of rotating and vibrating filtration for clarification of rough beer. *J Food Eng* 2007; 80: 206-17. <http://dx.doi.org/10.1016/j.jfoodeng.2006.05.022>
- [17] Sarkar P, Ghosh S, Dutta S, Sen D, Bhattacharjee C. Effect of different operating parameters on the recovery of proteins from casein whey using a rotating disc membrane ultrafiltration cell. *Desalin* 2009; 249: 5-11. <http://dx.doi.org/10.1016/j.desal.2009.06.007>
- [18] Taamneh Y, Ripperger S. Performance of single and double shaft disk separators. *Phys Separ. in Science and Eng* 2008; ID508617
- [19] Tu Z, Ding L. Microfiltration of mineral suspensions using a MSD module with rotating ceramic and polymeric membranes. *Separ Purif Technol* 2010; 73: 363-70. <http://dx.doi.org/10.1016/j.seppur.2010.04.024>
- [20] Luo J, Ding L, Wan Y, Paullier P, Jaffrin MY. Fouling behaviour of dairy wastewater treatment by nanofiltration under shear-enhanced extreme hydraulic conditions. *Sep Purif Technol* 2012; 88: 79-86. <http://dx.doi.org/10.1016/j.seppur.2011.12.008>

- [21] Luo J, Ding L, Wan Y, Jaffrin MY. Threshold flux for shear-enhanced nanofiltration: experimental observation in dairy wastewater treatment. *J Membr Sci* 2012; 409-10: 276-84. <http://dx.doi.org/10.1016/j.memsci.2012.03.065>
- [22] Bendick J, Reed B, Morrow P, Carole T. Using a high shear rotary membrane system to treat shipboard wastewaters: Experimental disk diameter, rotation and flux relationships. *J Membr Sci* 2014; 462: 178-84. <http://dx.doi.org/10.1016/j.memsci.2014.02.015>
- [23] Zhu Z, Luo J, Ding L, Bals O, Jaffrin MY, Vorobiev E. Chicory juice clarification by membrane filtration using rotating disk module. *J Food Eng* 2013; 115: 264-73. <http://dx.doi.org/10.1016/j.jfoodeng.2012.10.028>
- [24] Zhu Z, Ladeg S, Ding L, Bals O, Moulai-Mostefa N, *et al.* Study of rotating disk assisted dead-end filtration of chicory juice and its performance optimization. *Indus Crops and Products* 2014; 53: 154-62. <http://dx.doi.org/10.1016/j.indcrop.2013.12.030>
- [25] Ebrahimi M, Schmitz O, Kerker S, Lieberman F, Czermak P. Dynamic cross flow filtration of oil-field produced water by rotating ceramic filter discs. *Desalin and Water Treatment* 2013; 51: 1762-8. <http://dx.doi.org/10.1080/19443994.2012.694197>
- [26] Zhang W, Zhu Z, Jaffrin MY, Ding L. Effects of hydraulic conditions on effluent quality, flux behaviour, and energy consumption in a shear-enhanced membrane filtration using Box-Behnken response surface methodology. *Ind Eng Chem Res* 2014; 53(17) 71: 76-85.
- [27] Luo J, Zhu Z, Ding L, Bals O, Wan Y, Jaffrin MY, Vorobiev E. Flux behavior in clarification of chicory juice by high-shear membrane filtration: Evidence for threshold flux. *J Membr Sci* 2013; 435: 120-9. <http://dx.doi.org/10.1016/j.memsci.2013.01.057>
- [28] Rios SD, Salvado J, Farriol X, Torras C. Antifouling microfiltration strategies to harvest microalgae for biofuel. *Bioresources Tech* 2012; 119: 406-18. <http://dx.doi.org/10.1016/j.biortech.2012.05.044>
- [29] Shi W, Benjamin MM. Effect of shear rate on fouling in a vibratory shear enhanced processing VSEP RO system. *J Membr Sci* 2011; 366: 148-57. <http://dx.doi.org/10.1016/j.memsci.2010.09.051>
- [30] Ahmed S, Rasul MG, Hasib MA, Watanabe Y. Performance of a nanofiltration membrane in a vibrating module (VSEP-NF) for arsenic removal. *Desalin* 2010; 252: 127-34. <http://dx.doi.org/10.1016/j.desal.2009.10.013>
- [31] Zouboulis AI, Petala MD. Performance of VSEP vibratory membrane filtration system during the treatment of landfill leachates. *Desalination* 2008; 222: 165-75. <http://dx.doi.org/10.1016/j.desal.2007.01.145>
- [32] Subramani A, DeCarolis J, Pearce W, Jacangelo JG. Vibratory shear enhanced process (VSEP) for treating brackish water reverse osmosis concentrate with high silica content. *Desalination* 2012; 291: 15-22. <http://dx.doi.org/10.1016/j.desal.2012.01.020>
- [33] Kertesz S, Laszlo Z, Forgacs E, Szabo G, Hodur C. Dairy wastewater purification by vibratory enhanced processing. *Desal Water Treatment* 2011; 35: 195-201. <http://dx.doi.org/10.5004/dwt.2011.2485>
- [34] Gomaa HG, Rao S, Al-Taweel AM. Intensification of membrane microfiltration using oscillatory motion. *Sepur Purif Technol* 2011; 78: 336-44. <http://dx.doi.org/10.1016/j.seppur.2011.01.007>
- [35] Gomaa HG, Rao S, Al-Taweel AM. Flux enhancement using oscillatory motion and turbulent promoters. *J Membr Sci* 2011; 381: 64-73. <http://dx.doi.org/10.1016/j.memsci.2011.07.014>
- [36] Beier SP, Jonsson G. A vibrating membrane bioreactor (VMBR): Macromolecular transmission-influences of extracellular polymeric substances. *Chem Eng Sci* 2009; 64: 1436-44. <http://dx.doi.org/10.1016/j.ces.2008.12.008>
- [37] Yang X, Wang R, Fane AG, Tang CY, Wenten IG. Membrane module design and dynamic shear-induced techniques to enhance liquid separation by hollow fibers modules: a review. *Desalin Water Treatment* 2013; 51: 3604-27. <http://dx.doi.org/10.1080/19443994.2012.751146>